

Thermodynamic properties of ammonium haloplatinates

I. Heat capacity and thermodynamic functions of ammonium hexachloroplatinate $(\text{NH}_4)_2\text{PtCl}_6$ from 6 K to 348 K

RON D. WEIR,^a

*Department of Chemistry and Chemical Engineering,
Royal Military College of Canada,
Kingston, Ontario K7K 5L0, Canada*

and EDGAR F. WESTRUM, JR.

*Department of Chemistry, University of Michigan,
Ann Arbor, MI 48109–1055, U.S.A.*

(Received 17 April 1990; in final form 18 June 1990)

The heat capacity of ammonium hexachloroplatinate $(\text{NH}_4)_2\text{PtCl}_6$ was measured from 6 K to 348 K by adiabatic calorimetry. The heat-capacity curve is sigmoidal without anomalies. It rises rapidly from $T \rightarrow 0$ to 250 K where the $C_{p,m}/R$ value is 30.1 and increases by only 7 per cent from 250 K to 350 K. Values of the standard thermodynamic quantities are tabulated to 350 K.

1. Introduction

The metal salts of the family A_2MX_6 (A = an alkali metal, M = a transition metal or polyvalent ion, and X = a halogen) usually crystallize at room temperature into the cubic antiferroite structure of space group $\text{Fm}\bar{3}\text{m}$ or No. 225 O_h^5 . Depending upon chemical composition, some members of this family undergo structural phase transitions as the temperature is lowered and change into a phase of lower symmetry, while other members show no hint of a transition.^(1,2) In general, transition temperatures are shifted to lower values with increasing size of the cations and decreasing size of the hydrogen ligand. In some of the salts, the transitions involve the small-angle librations of the MX_6^{2-} octahedra, and in others the transitions lead to distortions of the cubic lattice without a coupling to the octahedral rotations.^(1–3) In K_2ReCl_6 , the transition at 109 K from cubic to the tetragonal structure is the displacive type driven by soft rotational modes.^(4,5)

^a To whom correspondence should be sent.

The substitution of the ammonium ion, either NH_4^+ or ND_4^+ , for the alkali metal leads to the introduction of additional librational degrees of freedom. In these $(\text{NH}_4)_2\text{MX}_6$ compounds, the structural phase transition is either suppressed or the transition temperature is lowered by the tetrahedral symmetry of the ammonium ion.⁽³⁾ In addition, when polyatomic anions are present, the distribution of charge on the anion over several atoms weakens the electrostatic attraction between any of these atoms and a hydrogen of an ammonium ion. This results in a low barrier height for rotation of either the NH_4^+ or ND_4^+ .

The stable cubic phase⁽⁶⁾ of ammonium hexafluorosilicate $(\text{NH}_4)_2\text{SiF}_6$ shows no transition in its crystal structure below room temperature and its heat capacity is without an anomaly from 25 K to 300 K.⁽⁷⁾ The barrier to rotation of the NH_4^+ is 1107 K based on n.m.r. results⁽⁸⁾ or 1616 K from heat capacities.⁽⁹⁾ The heat capacity of the deuterated analogue $(\text{ND}_4)_2\text{SiF}_6$, also without anomaly from 6 K to 343 K, yields a librational wavenumber of 122 cm^{-1} for the ND_4^+ ion.⁽¹⁰⁾ By comparison, the cubic $(\text{NH}_4)_2\text{SnCl}_6$ is also without any phase transition between room temperature and 20 K,⁽¹¹⁾ but has a much lower barrier to rotation of the ammonium ion which has been determined at 600 K to 740 K.^(8,9,12-14) However, the heat capacity of $(\text{ND}_4)_2\text{SnCl}_6$ shows a λ -shaped anomaly around 244 K. Whether its high-temperature cubic structure changes as the temperature is lowered below 244 K is so far not known.⁽¹⁵⁾

An even lower barrier to rotation of the NH_4^+ of 342 K has been reported⁽¹⁴⁾ in $(\text{NH}_4)_2\text{PtCl}_6$. As a result, interest has been attracted to determine the rotational potential of NH_4^+ in this compound,^(16,17) as well as in related ammonium hexachlorides.⁽¹⁸⁾ Heat-capacity results, a knowledge of which should assist in understanding the mechanism of molecular rotation, are unavailable for either $(\text{NH}_4)_2\text{PtCl}_6$ or its deuterated analogue. It is of historical interest that ammonium hexachloroplatinate $(\text{NH}_4)_2\text{PtCl}_6$ was the first coordination compound studied by X-ray diffraction.⁽¹⁹⁾ At room temperature, it has an antiferite-like structure of space group $\text{Fm}\bar{3}\text{m}$ (No. 225 O_h^5) with four formula units in the face-centred cell and $a_0 = 0.98580\text{ nm}$.^(20,21) Each NH_4^+ ion is coordinated with 12 equivalent Cl atoms at the corners of the unit cell and the hydrogen atoms within the NH_4^+ point towards empty corners as indicated in figure 1. Rotation of the NH_4^+ is indicated around both a twofold and a threefold axis. We have measured the heat capacity of $(\text{NH}_4)_2\text{PtCl}_6$ from 6 K to 350 K by adiabatic calorimetry as part of our ongoing work with ammonium salts, and the results are described below.

2. Experimental

The sample of $(\text{NH}_4)_2\text{PtCl}_6$ was supplied by the Aldrich Chemical Company as 99.999 mass per cent pure according to the Certificate of Analysis. No other elements were detected by spectrographic trace analysis at the detection level of mass fraction 1×10^{-6} . The finely divided yellow powder was used as supplied; there was no need to grind the sample further.

The Guinier-de Wolff diffraction pattern of our sample was in perfect agreement with the standard pattern for this compound: No. 7-218 as determined by the Joint

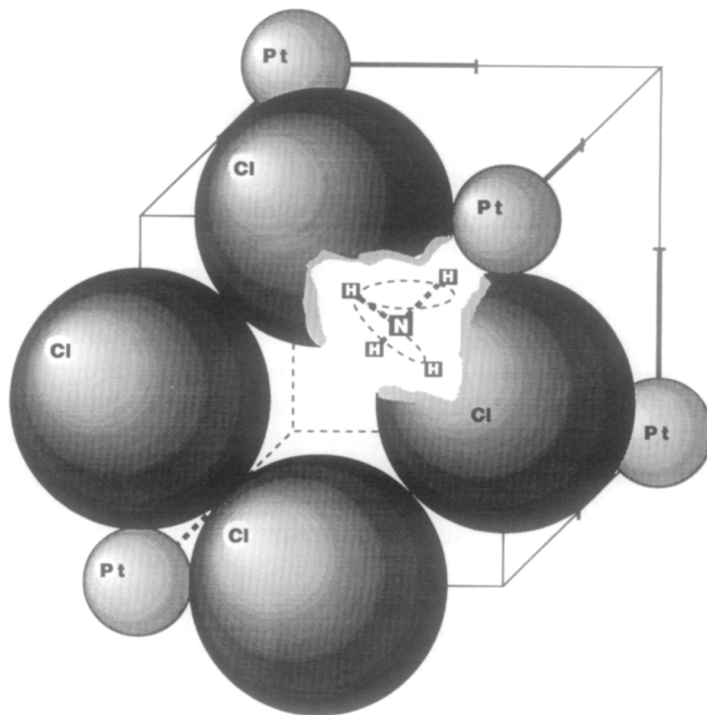


FIGURE 1. One-eighth of the unit cell of cubic $(\text{NH}_4)_2\text{PtCl}_6$ with side $a_0/2$. Approximate ionic radii are shown for Pt^{4+} and Cl^- , and the heavy lines denote the structure parameter $u = 0.24$ for Cl^- positions and the $\text{Pt}-\text{Cl}$ bond. Rotation of NH_4^+ about a two-fold and a three-fold axis is given.

Committee for Powder Diffraction Standards.⁽²⁰⁾ The structure is face-centred cubic at room temperature with $a = (0.9856 \pm 0.0001)$ nm.

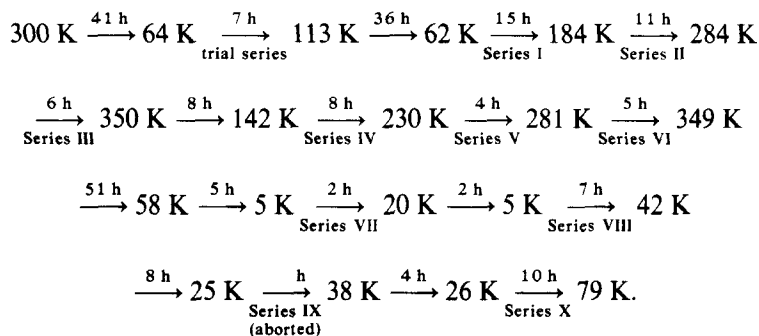
The molar heat capacity $C_{p,m}$ was measured from 6.3 K to 348 K in the Mark XIII adiabatic cryostat, which is an upgraded version of the Mark II cryostat described previously.⁽²²⁾ A guard shield was incorporated to surround the adiabatic shield. A Leeds and Northrup capsule-type platinum resistance thermometer (laboratory designation A-5) was used for temperature measurements. The thermometer was calibrated at the U.S. National Bureau of Standards (N.B.S.) against the IPTS-1948 (as revised in 1960)⁽²³⁾ for temperatures above 90 K, against the N.B.S. provisional scale from 10 K to 90 K, and by the technique of McCrackin and Chang⁽²⁴⁾ below 10 K. These calibrations are judged to reproduce thermodynamic temperatures to within 0.03 K between 10 K and 90 K and within 0.04 K above 90 K.⁽²⁵⁾ Measurements of mass, current, potential difference, and time were based upon calibrations done at N.B.S. The acquisition of heat capacities was assisted^(26, 27) by a computer programmed for a series of determinations. During the drift periods, both the calorimeter temperature and its first and second derivatives of temperature with respect to time were recorded to establish the equilibrium temperatures of the calorimeter between the energy inputs. During energy inputs, the heater current and

potential difference and the duration of the heating interval were obtained. Also recorded were the apparent heat capacity of the system including the calorimeter, heater, thermometer, and sample.

A gold-plated copper calorimeter (laboratory designation W-99) with four internal vertical vanes and a central entrant well for (heater + thermometer) was loaded with $(\text{NH}_4)_2\text{PtCl}_6$. After loading, the calorimeter was evacuated and pumping was continued for several hours to ensure that moisture was no longer released from the sample. After addition of about 2.5 kPa (at 300 K) of helium gas to the vessel to facilitate thermal equilibration, it was then sealed by means of an annealed gold gasket tightly pressed on to the stainless-steel knife edge of the calorimeter top with a screw closure about 5 mm in diameter.

Buoyancy corrections were calculated on the basis of a crystallographic density of $3.077 \text{ g}\cdot\text{cm}^{-3}$ derived from the unit cell edge of our sample. The mass of $(\text{NH}_4)_2\text{PtCl}_6$ was 6.447116 g, $\cong 0.01452429 \text{ mol}$ based on its molar mass of $443.88516 \text{ mol}^{-1}$ from IUPAC 1983 relative atomic masses.

The thermal history of the $(\text{NH}_4)_2\text{PtCl}_6$ is shown by the linear array. The solid arrows indicate cooling or heating, which correspond to acquisition of heat-capacity results.



3. Results and discussion

The experimental molar heat capacities for $(\text{NH}_4)_2\text{PtCl}_6$ are given in table 1. The standard errors in our heat capacity decrease from about 1 per cent at 10 K to less than 0.15 per cent at temperatures above 30 K. The heat capacity of the sample represented about (32 to 64) per cent of the measured total heat capacity.

A plot of $C_{p,m}/R$ against T from 6 K to 348 K is presented in figure 2. The curve is smooth and without anomalies. It rises rapidly from $T \rightarrow 0$ to 250 K. At that temperature, the $C_{p,m}/R$ value becomes 30.1 and increases more slowly over the next 10 K to a value of 32.0.

Special care was taken with respect to particle size and thermal history of our $(\text{NH}_4)_2\text{PtCl}_6$ sample in view of the hysteresis in $C_{p,m}$ encountered by other workers with various ammonium compounds, but not necessarily with ammonium hexachloroplatinate. Reproducibilities of the heat-capacity values of NH_4PF_6 ,

TABLE 1. Experimental molar heat capacity of $(\text{NH}_4)_2\text{PtCl}_6$
($M = 443.88516 \text{ g} \cdot \text{mol}^{-1}$; $R = 8.31451 \text{ J} \cdot \text{K}^{-1} \cdot \text{mol}^{-1}$)

T/K	$C_{p,m}/R$	T/K	$C_{p,m}/R$	T/K	$C_{p,m}/R$	T/K	$C_{p,m}/R$	T/K	$C_{p,m}/R$
Series I		Series II		343.32	31.81	Series VI		14.74	1.574
65.43	14.61	187.11	28.05	347.75	31.96	288.56	30.52	15.84	1.906
70.96	15.85	192.47	28.11	Series IV		293.63	30.53	17.36	2.366
76.02	16.87	197.77	28.30	148.93	25.96	298.62	30.69	18.87	2.818
80.86	17.63	202.97	28.55	153.67	26.40	303.59	30.63	20.43	3.287
85.33	18.33	208.10	28.79	162.96	26.89	308.55	39.89	22.01	3.737
89.46	19.22	213.19	28.98	167.50	27.14	313.49	30.93	23.87	4.308
92.74	19.58	218.24	29.17	172.00	27.38	318.42	31.11	26.05	4.897
96.76	20.41	228.27	29.63	176.58	27.58	323.32	31.28	28.07	5.407
100.61	21.07	233.27	29.68	181.11	27.77	328.23	31.39	Series X	
104.35	21.57	243.05	30.05	185.49	27.97	333.13	31.52	30.45	6.085
108.51	22.04	247.92	30.00	194.38	28.33	338.03	31.66	35.41	7.463
113.05	22.60	252.77	30.15	198.88	28.35	343.09	31.79	38.40	8.179
117.42	23.14	257.61	30.12	203.24	28.63	347.40	32.03	41.50	8.949
121.69	23.63	262.41	30.30	207.50	28.82	Series VII		44.77	9.697
125.88	23.98	267.20	30.25	211.74	28.94	6.44	0.123	48.20	10.60
129.99	24.47	271.95	30.34	215.94	29.02	7.56	0.219	50.97	11.25
134.03	24.81	276.70	30.37	220.14	29.28	8.26	0.290	55.18	12.26
138.01	25.21	281.44	30.50	224.30	29.37	9.07	0.387	59.12	13.19
141.94	25.48	Series III		228.44	29.52	Series VIII		63.11	14.11
145.82	25.79	291.56	30.55	Series V		6.34	0.115	67.38	15.05
149.66	26.12	296.70	30.63	243.53	29.95	7.18	0.182	71.92	16.01
153.46	26.42	301.86	30.72	248.65	30.05	7.76	0.238	76.49	16.93
157.22	26.58	307.02	30.79	253.75	30.03	8.59	0.327		
160.95	26.67	312.22	30.96	258.90	30.24	9.46	0.444		
164.63	26.95	317.49	31.17	263.99	30.31	10.32	0.579		
168.28	27.20	322.67	31.37	268.99	30.38	12.34	0.947		
171.91	27.37	327.72	31.45	273.98	30.32	13.29	1.170		
175.50	27.58	332.92	31.64	278.97	30.45	14.08	1.375		
182.63	27.84	338.11	31.69						

RbPF_6 , $(\text{NH}_4)_2\text{SnCl}_6$, K_2SnCl_6 , and Rb_2SnCl_6 were all found to be dependent on particle size, which in turn was affected by thermal history.^(28,29) In an n.m.r. study of KPF_6 and RbPF_6 ,⁽³⁰⁾ the temperature dependence of the fluorine resonance also depended on particle size and previous physical treatment. Reproducible results were obtained on samples in the form of fine powders. Those that were crystalline before their first cooling showed hysteresis and the process of cooling and warming broke up the crystallites into small particles thereby eliminating the effects of hysteresis. Our $(\text{NH}_4)_2\text{PtCl}_6$ sample was supplied as a finely divided powder and it was cooled to 64 K, warmed to 113 K, and cooled again to 62 K before the heat-capacity results were begun. No hysteresis is apparent between the $C_{p,m}$ values in our multiple series of runs.

Integration of the smoothed values for heat capacity and for the enthalpy and entropy increments yielded the thermodynamic functions. Values of $C_{p,m}/R$ and the derived functions are presented at selected temperatures in table 2. The heat capacities of $(\text{NH}_4)_2\text{PtCl}_6$ below 6 K were obtained by fitting our experimental values below 20 K to the limiting form of the Debye equation, with a plot of $C_{p,m}/T^3$

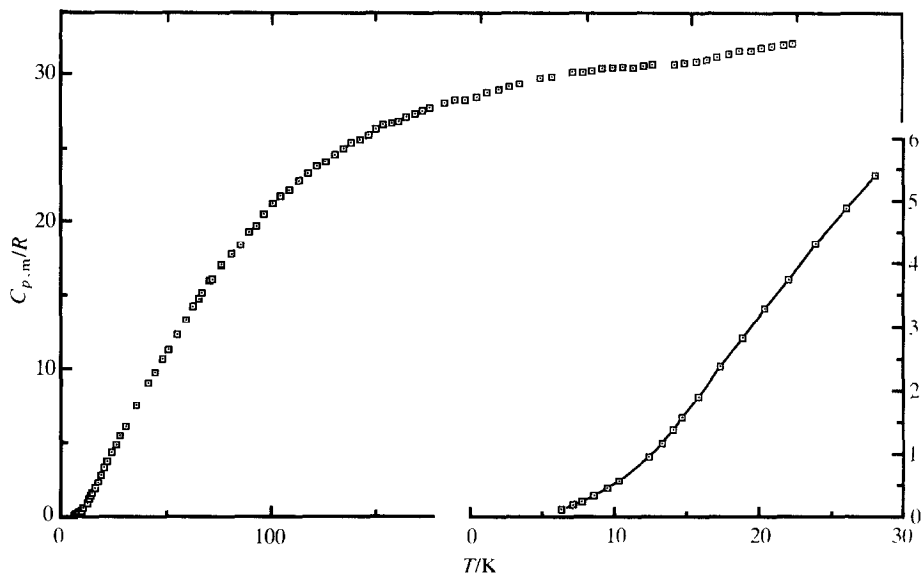


FIGURE 2. Experimental molar heat capacities $C_{p,m}$ at constant pressure plotted against temperature T for $(\text{NH}_4)_2\text{PtCl}_6$. The region below 20 K is enlarged in the lower right-hand corner.

against T^2 extrapolated to $T \rightarrow 0$, shown in figure 3. Such a plot is also useful for identifying any non-vibrational contributions to the heat capacity at low temperatures. Although the quantity measured calorimetrically is $C_{\text{sat},m}$, it effectively equals $C_{p,m}$ for these solids. In addition, the correction of $C_{p,m}$ to $C_{v,m}$, which is needed for analysis of any heat-capacity results, is negligible at these low temperatures so that the heat capacity of our $(\text{NH}_4)_2\text{PtCl}_6$ insulator, can be written as a power series:

$$C_{p,m} = C_{v,m} = aT^3 + bT^5 + cT^7 + \dots \quad (1)$$

Here, the coefficients a , b , and c are directly related to the corresponding power series for the frequency spectrum at low frequencies.⁽³¹⁾ Thus as $T \rightarrow 0$, the lattice heat-capacity of the solid should become equal to that of an elastic continuum and can be described by the Debye " T^3 " law:

$$C_{v,m} = aT^3, \quad (2)$$

and

$$\Theta_0^C = (12\pi^4 Lk/5a)^{1/3}. \quad (3)$$

The Θ_0^C is the Debye characteristic temperature derived from heat capacities. In our figure 3, in the region $36 < (T^2/\text{K}^2) < 400$ {i.e. $6 < (T/\text{K}) < 20$ }, the experimental heat capacities for $(\text{NH}_4)_2\text{PtCl}_6$ follow a curve similar in shape to that for argon and suggest that only lattice vibrations make significant contributions to the heat capacity in this temperature range. Extrapolation of the points below $T^2 = 36 \text{ K}^2$ in figure 3 to intercept the $T^2 = 0$ axis at a/R gives $10^4 a/R = (3.98 \pm 0.13) \text{ K}^3$ or

TABLE 2. Standard molar thermodynamic functions for (ND₄)₂PtCl₆

$$M = 443.88516 \text{ g} \cdot \text{mol}^{-1}, p^\circ = 101.325 \text{ kPa}, R = 8.31451 \text{ J} \cdot \text{K}^{-1} \cdot \text{mol}^{-1}, \Phi_m^{\circ} = \Delta_0^{\circ} S_m^{\circ} - \Delta_0^{\circ} H_m^{\circ} / T$$

<i>T</i> K	<i>C</i> _{p,m} <i>R</i>	$\frac{\Delta_0^{\circ} S_m^{\circ}}{R}$	$\frac{\Delta_0^{\circ} H_m^{\circ}}{R \cdot K}$	$\frac{\Phi_m^{\circ}}{R}$	<i>T</i> K	<i>C</i> _{p,m} <i>R</i>	$\frac{\Delta_0^{\circ} S_m^{\circ}}{R}$	$\frac{\Delta_0^{\circ} H_m^{\circ}}{R \cdot K}$	Φ_m° <i>R</i>
0	0	0	0	0	150	26.14	27.87	2244.9	12.91
5	(0.0550)	(0.0178)	(0.0689)	(0.0040)	155	26.44	28.73	2376.4	13.40
10	0.527	0.165	1.27	0.038	160	26.73	29.58	2509.3	13.90
15	1.660	0.559	6.32	0.137	165	27.00	30.41	2643.6	14.38
20	3.170	1.247	18.47	0.323	170	27.27	31.22	2779.3	14.87
25	4.615	2.112	38.01	0.592	175	27.51	32.01	2916.2	15.35
30	5.965	3.072	64.45	0.924	180	27.71	32.79	3054.3	15.82
35	7.360	4.095	97.72	1.303	185	27.90	33.55	3193.3	16.29
40	8.565	5.157	137.6	1.718	190	28.07	34.30	3333.2	16.75
45	9.798	6.237	183.5	2.160	195	28.24	35.03	3474.0	17.21
50	11.03	7.333	235.5	2.622	200	28.39	35.74	3615.6	17.67
55	12.23	8.440	293.7	3.100	205	28.64	36.45	3758.2	18.12
60	13.40	9.554	357.7	3.592	210	28.87	37.14	3901.9	18.56
65	14.53	10.67	427.6	4.093	215	29.08	37.82	4046.8	19.00
70	15.65	11.79	503.0	4.603	220	29.28	38.49	4192.7	19.44
75	16.65	12.90	583.8	5.119	225	29.47	39.15	4339.6	19.87
80	17.55	14.01	669.3	5.640	230	29.65	39.80	4487.4	20.29
85	18.38	15.10	759.1	6.165	240	29.93	41.07	4786.3	21.13
90	19.22	16.17	853.0	6.691	250	30.13	42.30	5085.7	21.96
95	20.11	17.23	951.3	7.218	260	30.23	43.48	5387.5	22.76
100	21.00	18.29	1054.1	7.745	270	30.34	44.63	5690.5	23.55
105	21.63	19.33	1160.7	8.272	280	30.44	45.73	5994.4	24.32
110	22.24	20.35	1270.3	8.798	290	30.55	46.80	6299.4	25.08
115	22.84	21.35	1383.0	9.322	300	30.67	47.84	6606.5	25.82
120	23.43	22.33	1499.7	9.843	310	30.94	48.85	6913.5	26.55
125	23.96	23.30	1617.1	10.36	320	31.20	49.84	7224.2	27.26
130	24.45	24.25	1738.1	10.88	330	31.47	50.80	7537.6	27.96
135	24.92	25.18	1861.5	11.39	340	31.76	51.74	7853.7	28.64
140	25.37	26.10	1987.3	11.90	350	32.03	52.67	8172.7	29.32
145	25.78	26.99	2155.1	12.41	298.15	30.65	47.65	6548.7	25.68
						±0.03	±0.05	±6.5	±0.03

$10^4 a = (33.1 \pm 1.1) \text{ J} \cdot \text{K}^{-1} \cdot \text{mol}^{-1}$, which yields from equation (3) $\Theta_0^C = (83.7 \pm 1.0) \text{ K}$. This compares with 93.5 K for argon.

The results of n.m.r. experiments for (NH₄)₂PtCl₆ over the range from 55 K to room temperature show that: NH₄⁺ reorientation dominates the relaxation between 55 K and 250 K; PtCl₆⁻ reorientation begins to contribute to the relaxation above 140 K; and the derived activation energy $\Delta^{\ddagger}U_m^{\circ}$ for NH₄⁺ reorientation is $1590 \text{ J} \cdot \text{mol}^{-1}$.⁽³²⁾ This value of $\Delta^{\ddagger}U_m^{\circ}$ is substantially lower than the $2845 \text{ J} \cdot \text{mol}^{-1}$ determined in reference 14. Additional light was shed on the NH₄⁺ reorientation in (NH₄)₂PtCl₆ by another n.m.r. study over a wider temperature range than previously reported. In this work from 4 K to 296 K,⁽³³⁾ both the proton spin relaxation *T*₁ in the laboratory frame and the *T*_{1ρ} in the rotating frame were not linear over the entire temperature region. Use of the semiclassical model of NH₄⁺ rotation fails to predict the minima found in *T*₁ and *T*_{1ρ}. By considering the splitting of the proton spins into

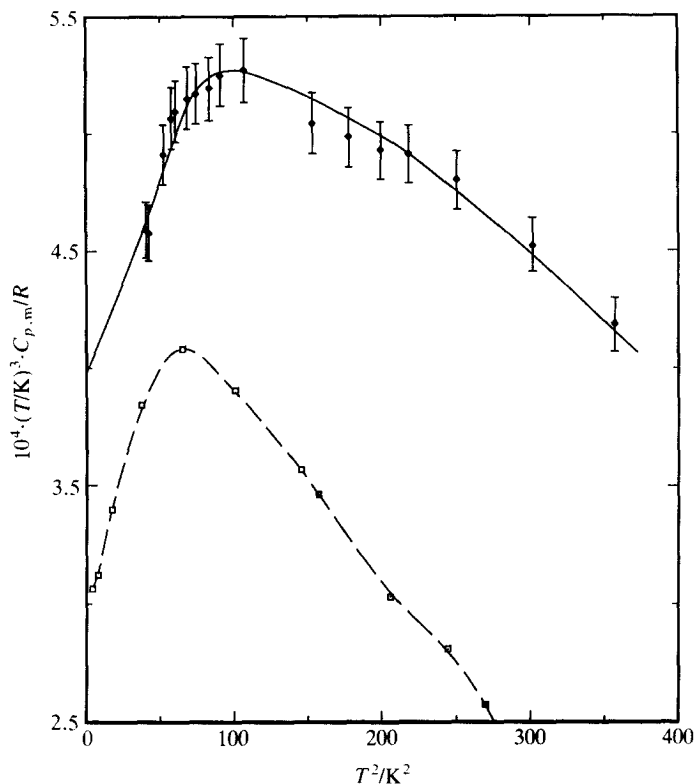


FIGURE 3. Experimental values of $C_{p,m}/RT^3$ plotted against T^2 for $(\text{NH}_4)_2\text{PtCl}_6$: —, this work; ---, argon (references 37, 38).

one A-symmetry state with nuclear spin $I = 2$, three degenerate T states with $I = 1$, and two degenerate E states with $I = 0$, and by applying the methods of Haupt⁽³⁴⁾ to the NH_4^+ group for spin-lattice relaxation in the presence of quantum-mechanical tunnelling through hindered barriers, a qualitative explanation of the proton relaxation in $(\text{NH}_4)_2\text{PtCl}_6$ is provided. For both $(\text{NH}_4)_2\text{PtCl}_6$ and $(\text{NH}_4)_2\text{PtBr}_6$, spin isomerism for NH_4^+ is necessary to explain the n.m.r. results, but tunnelling provides the dominant relaxation at the lowest temperatures studied only for $(\text{NH}_4)_2\text{PtCl}_6$.⁽³³⁾ Tunnelling frequencies for the NH_4^+ motion in the hexachlorides are too large for two-fold sinusoidal barriers.⁽¹⁴⁾ The NH_4^+ torsional motion in $(\text{NH}_4)_2\text{PtCl}_6$ appears to be in box-like potentials⁽³⁵⁾ with reorientation over three-fold barriers.⁽¹⁶⁾ The rotation of NH_4^+ about the three-fold axis is shown in figure 1. Box-like potentials with minima away from the axes of symmetry were also found by neutron diffraction in the proton distribution in isostructural $(\text{NH}_4)_2\text{SiF}_6$.⁽³⁶⁾

We thank Dr R. D. Heyding for determining the crystal structure of our sample. One of us (R.D.W.) thanks the Department of National Defence (Canada) for financial support.

REFERENCES

1. Rössler, K.; Winter, J. *Chem. Phys. Lett.* **1977**, *46*, 566.
2. Armstrong, R. L. *Phys. Rep.* **1980**, *57*, 343.
3. Regelsberger, M.; Pelz, J. *Solid State Comm.* **1978**, *28*, 783.
4. O'Leary, G. P.; Wheeler, R. G. *Phys. Rev.* **1970**, *B1*, 4409.
5. Lynn, J. W.; Patterson, H. H.; Shirane, G.; Wheeler, R. G. *Solid State Comm.* **1978**, *27*, 859.
6. Marignac, M. *Ann. Mines* **1857**, *12*, 19.
7. Stephenson, C. C.; Wulff, C. A.; Lundell, O. R. *J. Chem. Phys.* **1964**, *40*, 967.
8. Strange, J. H.; Terenzi, M. J. *Phys. Chem. Solids* **1972**, *33*, 923.
9. Smith, D. *Chem. Phys. Lett.* **1974**, *25*, 348.
10. Smith, D.; Weir, R. D.; Westrum, E. F., Jr. *J. Chem. Thermodynamics* **1990**, *22*, 421.
11. Morphee, R. G. S.; Staveley, L. A. K.; Walters, S. T.; Wigley, D. L. *J. Phys. Chem. Solids* **1960**, *13*, 132.
12. Svare, I. *J. Phys. C: Solid State Phys.* **1977**, *10*, 4137.
13. Prager, M.; Press, W.; Alefield, B.; Hüller, A. *J. Chem. Phys.* **1977**, *67*, 5126.
14. Svare, I.; Raaen, A. M.; Thorkildsen, G. *J. Phys. C: Solid State Phys.* **1978**, *11*, 4069.
15. Callanan, J. E.; Weir, R. D.; Westrum, E. F., Jr. *J. Chem. Thermodynamics* **1990**, *22*, 149.
16. Otnes, K.; Svare, I. *J. Phys. C: Solid State Phys.* **1979**, *12*, 3899.
17. Hoser, A.; Prandl, W.; Heger, G. *Proceedings ILL-IFF Workshop on Quantum Aspects of Molecular Motions in Solids*. Heidemann, A.; Magerl, A.; Prager, M.; Richter, D.; Springer, T.: editors. Springer: Berlin. **1986**, pp. 19–23.
18. Smith, D. *J. Chem. Phys.* **1985**, *82*, 5133.
19. Wyckoff, R. W. G.; Posnjak, E. W. *J. Am. Chem. Soc.* **1921**, *43*, 2292.
20. Swanson, H. E.; Gilfrich, N. T.; Ugrinic, G. M. *Natl. Bur. Stand. (U.S.), Circ. No. 539*. **1955**, *5*, pp. 3–4.
21. Wyckoff, R. W. G. *Crystal Structures. Vol. 3*. Interscience: New York. **1965**, p. 342.
22. Westrum, E. F., Jr.; Furukawa, G. T.; McCullough, J. P. *Experimental Thermodynamics, Vol. 1*. McCullough, J. P.; Scott, D. W.: editors. Butterworths: London. **1968**, p. 133.
23. Stimson, H. F. *J. Res. Natl. Bur. Stand.* **1961**, *65A*, 139.
24. McCrackin, F. L.; Chang, S. S. *Rev. Sci. Instrum.* **1975**, *46*, 550.
25. Chirico, R. D.; Westrum, E. F., Jr. *J. Chem. Thermodynamics* **1980**, *12*, 311.
26. Westrum, E. F., Jr. *Proceedings NATO Advanced Study Institute on Thermochemistry, Viana do Castelo, Portugal*. Ribeiro da Silva, M. A. V.: editor. Reidel: New York. **1984**, p. 745.
27. Andrews, J. T. S.; Norton, P. A.; Westrum, E. F., Jr. *J. Chem. Thermodynamics* **1978**, *10*, 949.
28. Staveley, L. A. K.; Grey, N. R.; Layzell, M. J. *Z. Naturforsch.* **1963**, *18A*, 148.
29. Morphee, R. G. S.; Staveley, L. A. K. *Nature* **1957**, *180*, 1246.
30. Miller, G. R.; Gutowsky, H. S. *J. Chem. Phys.* **1963**, *39*, 1983.
31. Barron, T. H. K.; Berg, W. T.; Morrison, J. A. *Proc. Roy. Soc. London* **1957**, *A242*, 478.
32. Bonari, M.; Terenzi, M. *Chem. Phys. Lett.* **1974**, *27*, 281.
33. Armstrong, R. L.; Van Driel, H. M.; Sharp, A. R. *Can. J. Phys.* **1974**, *52*, 369.
34. Haupt, J. *Z. Naturforsch.* **1971**, *A26*, 1578.
35. Prager, M.; Raaen, A. M.; Svare, I. *J. Phys. C: Solid State Phys.* **1983**, *16*, L181.
36. Schlemper, E. O.; Hamilton, W. C.; Rush, J. J. *J. Chem. Phys.* **1966**, *44*, 2499.
37. Beaumont, R. H.; Chihara, H.; Morrison, J. A. *Proc. Phys. Soc. London* **1961**, *78*, 1462.
38. Finegold, L.; Phillips, N. E. *Phys. Rev.* **1969**, *177*, 1383.